

Effect of Proinflammatory Activation on F-Actin Distribution in Cultured Human Endothelial Cells under Conditions of Experimental Microgravity

E. G. Rudimov, S. V. Buravkov*, E. P. Andreeva, and L. B. Buravkova

Translated from *Kletochnye Tekhnologii v Biologii i Meditsine*, No. 4, pp. 260-267, October, 2014
Original article submitted October 15, 2013

We compared the state of actin cytoskeleton, morphology, and expression of VE-cadherin in endothelial cells of human umbilical cord vein under conditions of TNF- α -mediated activation and microgravity modeling and found that 3D-clinorotation for 24 h impaired the integrity of endothelial monolayer, altered cell morphology, induced cytoskeleton reorganization, and reduced the expression of VE-cadherin. The combination of experimental microgravity and proinflammatory activation led to more pronounced clearing of the perinuclear space from microfilaments and accumulation of depolymerized actin, which confirms additive effect of the studied factors on actin cytoskeleton of endothelial cells.

Key Words: *endothelial cells; microgravity; proinflammatory activation; cytoskeleton*

Structural and functional properties of cells can be modulated by various mechanical factors (mechanotransduction) including gravity, a mechanical stimulus that persistently acts on all living systems. During recent decades, some cellular modifications observed under conditions of microgravity were described [7,16,21,36,38]. Space experiments have demonstrated cytoskeleton rearrangement, loss of T cell activation, induction of apoptosis, and changed pattern of gene expression [9,17,33,35]. However, the intracellular mechanisms mediating the influence of gravitation factor remain unclear [2,20].

A good model for studying the mechanisms of mechanotransduction are endothelial cells (EC) lining the luminal surface of blood vessels *in vivo*; they represent the major barrier between the blood and adjacent tissues and function as a mechanosensitive interface for signal transduction (pressure, tension, contraction, shear stress) [25,28,32]. Moreover, EC play an important role in the maintenance of functional integrity of the vascular wall due to formation

of cell–cell adhesion contacts consisting of cadherin family proteins: endothelium-specific VE-cadherin (vascular endothelium cadherin, CD144, cadherin-5) and neural cadherin (N-cadherin) present in neural and muscular cells [8]. Similar to other cadherins, VE-cadherin binds via its cytoplasmic domain to adhesion contact proteins p120, β -catenin, and plakoglobin. They, in turn, bind to α -catenin that interacts with several actin-binding proteins (α -actinin, Ajuba, ZO-1, *etc.*) [37]. Thus, the cadherin complex is linked to actin cytoskeleton, but the molecular mechanisms of this interaction are poorly studied. It was thought that the contact with actin filaments is mediated by α -catenin, but further studies have demonstrated that α -catenin cannot bind to actin and β -catenin simultaneously [37]. At the same time, binding of VE-cadherin with catenins and actin is important for endothelium permeability and stabilization of cell contacts. Thus, mutation in gene encoding VE-cadherin in mice led to fetal death due to enhanced vascular permeability [13].

It can be now accepted that in EC, similar as in all other adherent cultures, cytoskeleton not only plays the structural function, but also acts as a converter of mechanical influences into cellular biochemical stimuli [14,15,22]. It has been reported that short-term clinostat

Institute of Biomedical Problems, Russian Academy of Sciences, Moscow; *M. V. Lomonosov Moscow State University, Russia. **Address for correspondence:** rydimov@gmail.com. E. G. Rudimov

exposure induced reorganization of actin skeleton in EC [10,20], while longer exposure led to re-adaptation of the endothelium to changed gravity [3].

The functional state of EC is largely determined by the influence of proinflammatory cytokines. TNF- α is a potent activator of proinflammatory properties of the endothelium: addition of this cytokine to the culture medium induces endothelial dysfunction manifesting at the early stages by enhanced expression of adhesion molecules ICAM, VCAM-1, and E-selectin [31]. Similar effect can be induced by TNF- α in low (10^{-9} g/ml) concentrations [24], whereas high concentrations of this cytokine induce apoptotic cell death [23]. However, the effect of experimental microgravity on functionally modulated EC, in particular, activated by proinflammatory cytokine TNF- α , remains obscure.

Here we studied organization of F-actin and expression of VE-cadherin in intact and preactivated human EC under conditions of modeled microgravity.

MATERIALS AND METHODS

Intact and activated EC from human umbilical cord vein (passages 2-4) were used in the experiments. Isolation of EC from human umbilical cord vein was carried out according to the well-known method with some modifications [1]. The cells were activated by incubation with 2 ng/ml TNF- α (BD Biosciences) for 6 and 24 h [31]. The cells were cultured in medium 199 (Gibco) containing 25 mM HEPES (MP Biomedicals), 10,000 U/ml penicillin and 10,000 μ g/ml streptomycin in 0.85% saline (PanEko), 1 mM sodium pyruvate (Gibco), 10% fetal calf serum (FCS; HyClone), 5 U/ml heparin, and 100 μ g/ml ECGS (BTI). The primary EC culture that attained monolayer was treated with trypsin (0.05%) and EDTA (0.02%; Gibco), transferred into 9- and 25-cm² flasks (Nunc), and cultured until confluence. Immediately before the experiment, the medium in flasks was replaced with a fresh portion; the flasks were completely filled with culture medium without air bubbles. The cell cultures were studied in two series: static control grown under standard conditions in a CO₂ incubator and cultures subjected to microgravity modeling using a Random Positioning Machine (RPM; Dutch Space) at a rate of 100 rad/min for the external and 80 rad/min for the internal frames for 6 and 24 h in a thermostat at 37°C. During rotation in RPM, the position of the object is randomly changed relative to the gravity vector due to randomized movement of perpendicular frames to which the platform with experimental samples is attached; this rotation allows reducing the influence of gravity of cells *in vitro* [34]. In the clinostat, the culture medium is constantly agitated; therefore, we used a shaker to control the effect of medium agitation.

F-actin structures were visualized using a standard TRITC-phalloidine dye (Sigma). To this end, the cells washed from the medium were fixed in 4% paraformaldehyde for 15 min. The cells were permeabilized with detergent 0.1% Triton X-100 (Sigma) that was added to prefixed cells for 15 min and then washed twice with PBS. Then, the cells were incubated for 40 min TRITC-phalloidine (50 μ g/ml) for 37°C and then washed with PBS. For protection of fluorescence, the preparations were embedded in a special water-soluble medium setting solid after application and containing blue DNA dye DAPI (Sigma). Changes in the structure of actin microfilaments were assessed by fluorescence microscopy on a confocal microscope LSM 780 (Carl Zeiss).

The expression of VE-cadherin was measured by indirect immunocytochemical staining with antibodies to VE-cadherin (Millipore) and FITC-labeled secondary antibody (Sigma) or using Vectastain ABC and DAB Peroxidase kits (Vector Laboratories). The preparations were analyzed under a Nikon Eclipse TiU or LSM 780 microscope (Carl Zeiss). The cells expressing VE-cadherin were determined by flow cytometry on an Epics XL flow cytometer (Beckman Coulter).

The data were processed statistically using Microsoft Excel and Statistica 7.0 software; the means and standard deviations were calculated. Significance of differences between two data sets was evaluated using nonparametric Mann-Whitney test ($p \leq 0.05$).

RESULTS

In the control series, intact cells cultured under static conditions were used (Fig. 1, *a*). Proinflammatory activation was evaluated by stimulation of the expression of immunoglobulin ICAM-1 on the cell surface, because the expression of this cell adhesion molecule sharply increases in few hours and after EC activation (Fig. 1, *b*) [27]. The results showed that addition of TNF- α to the incubation medium for 6 h resulted in a 2-fold increase in the content of ICAM-1⁺ cells, while 24-h incubation with the cytokine increased the relative content of ICAM-1⁺ cells by 5 times. Significant changes were noted only after 24-h incubation (Fig. 1, *c*). Therefore, 24-h incubation of EC with TNF- α was used in further experiments on evaluation of activation effect.

Proinflammatory activation of cells (Fig. 2, *b*) induced no appreciable changes in EC morphology in comparison with intact cells (Fig. 2, *a*). Randomization of the gravity vector over 24 h led to impairment of the integrity of endothelial monolayer and modified cell morphology (Fig. 2, *c*). After combination of modeled microgravity with proinflammatory activation, the

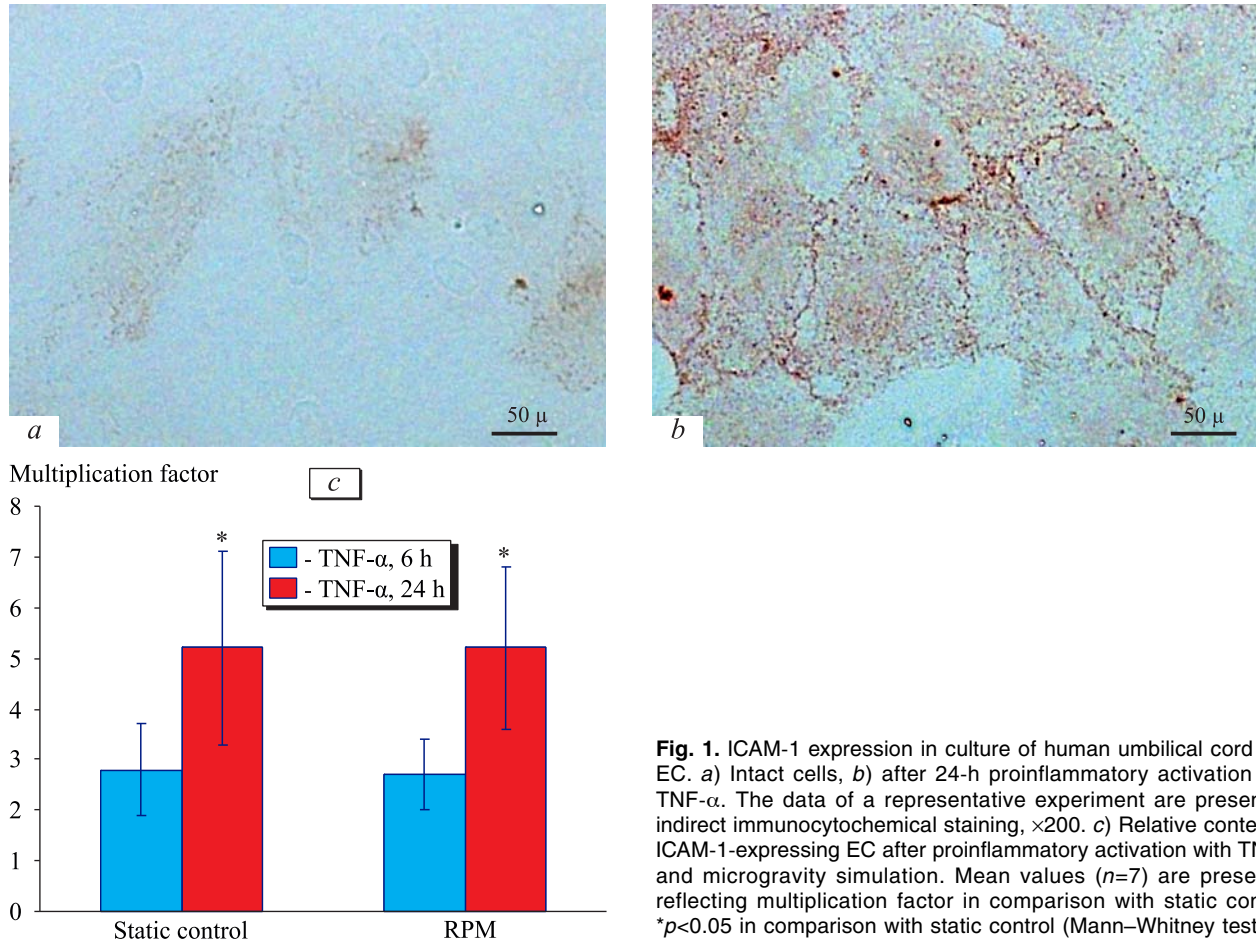


Fig. 1. ICAM-1 expression in culture of human umbilical cord vein EC. *a*) Intact cells, *b*) after 24-h proinflammatory activation with TNF- α . The data of a representative experiment are presented, indirect immunocytochemical staining, $\times 200$. *c*) Relative content of ICAM-1-expressing EC after proinflammatory activation with TNF- α and microgravity simulation. Mean values ($n=7$) are presented reflecting multiplication factor in comparison with static control. * $p < 0.05$ in comparison with static control (Mann–Whitney test).

changes observed in 3D-clinostasis (RPM) were more pronounced: the cells were more flattened and changed their shape due to formation of processes, lamella; the monolayer integrity was disturbed. In addition, considerable changes were noted in the cell cytosol: appearance of vacuole-like structures and clear-cut granularity in the perinuclear space (Fig. 2, *d*).

Analysis of changes in the organization of fibrillary actin filaments in EC showed that actin in intact EC was concentrated along the periphery of the cell in the form of thin filaments crossing its center (Fig. 3, *a*). At the same time, TNF-activation of cells and simulation of microgravity led to reorganization of the actin cytoskeleton, and these changes had complex nature (Fig. 3, *b*, *c*). In activated cells, the content of actin microfilaments increased. Many cells formed lamellopodia (Fig. 3, *f*) and filopodia (Fig. 3, *e*) primarily in areas of cell–cell contacts. These changes were accompanied by thickening of actin bundles followed by the formation of stress fibers. In most cells, the F-actin stress-fibers were arranged parallel to the long (main) axis of the cell. In addition, stellate structures, probably representing depolymerized actin lumps appeared in the area of cell–cell contacts.

Under the effect of simulated microgravity, EC became less flattened, which impaired the integrity of cell monolayer. In contrast to TNF- α -activated cells, these cells did not form filopodia, while stress-fibers were primarily located in sites of cell–cell contacts. This was always associated with fibril contraction and shrinkage of neighboring cells (Fig. 3, *c*).

These data agree with the results of previous analysis of morphological, biochemical, and dynamic changes in EC in response to TNF- α [30]. The combination of proinflammatory activation and 24-h RPM exposure potentiated this effect: characteristic “emptiness” appeared in the perinuclear space due to clearing of the cell center from microfilaments; the content of depolymerized actin significantly increased under these conditions (Fig. 3, *d*). These findings correlate with the results obtained in experiments with 2D-clinostasis of EC [10].

Reorganization of F-actin was associated with changes in the expression of VE-cadherin (CD144). When studying the effect of various factors on the relative content of CD144⁺ cells we found that TNF- α -activation of EC slightly increased this parameter (Fig. 4), whereas microgravity simulation reduced

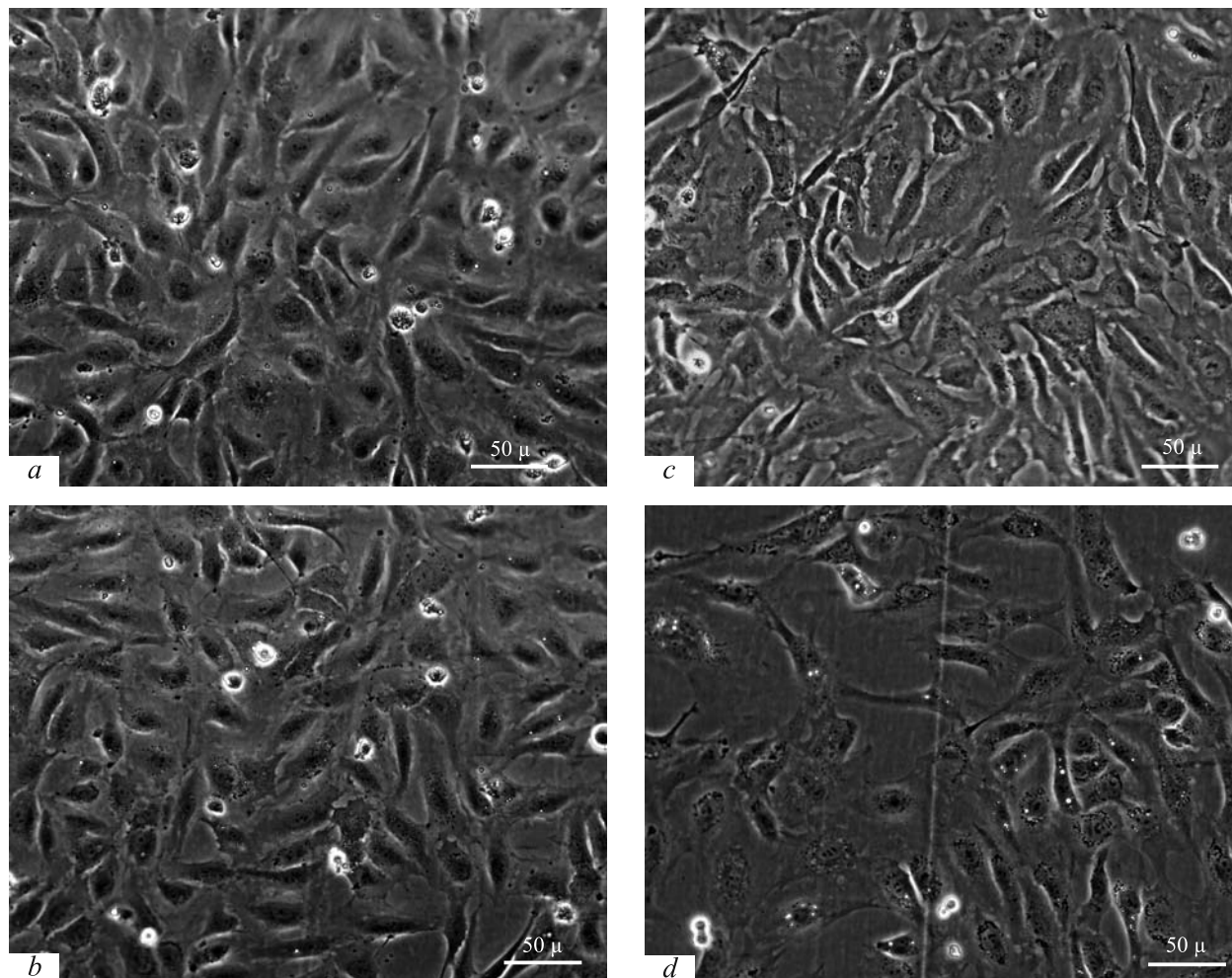


Fig. 2. Morphological peculiarities of endothelium *in vitro*: static control (a); EC activation with TNF- α (b); RPM exposure for 24 h (c); TNF- α activation+24-h RPM exposure (d). Phase-contrast microscopy, $\times 100$.

the percent of these cells. The number of activated CD144⁺ cells exposed to microgravity was significantly lower than the number of activated control cells, which probably suggests that this parameter did not depend on proinflammatory activation. It should be noted that RPM exposure was associated with the appearance of breaks of cell–cell contacts and inhibition of VE-cadherin expression (Fig. 5). This effect was observed as soon as in 6 h and remained at this level throughout the experiment.

These results are consistent with the reports of other researchers who have found that increasing permeability of endothelial monolayer under conditions of proinflammatory activation was caused by the appearance of specific breaks of cell–cell contacts due to TNF- α -mediated phosphorylation of VE-cadherin, rather than reduced expression of this glycoprotein [26]. However, our findings indicate that changes in the actin cytoskeleton architecture can be related to VE-cadherin distribution in the cell membrane. It can be hypothesized that VE-cadherin molecules remained

only in sites of cell–cell contacts, which was confirmed by reduced expression of this protein on the cell surface (Fig. 5).

Thus, EC were highly sensitive to mechanical stress, which was confirmed by the previous data [5,12,20], the plasma membrane and cytoskeleton being the most susceptible to mechanical stimulation structures [15]. A number of papers described changes in the spatial organization of microfilaments, intermediate filaments, and microtubules under conditions of space flight and ground-based experiments with simulated microgravity. The most convincing data indicate that F-actin microfilaments are the basic structure responsible for signal transmission. For instance, inhibition of mechanosensitive ionic channels in response to deformation occurs due to depolarization of actin microfilaments [36]. Hence, F-actin can be responsible for gravitational sensitivity of the endothelium that has been demonstrated in earlier studies [6]. For instance, cell exposure on a 2D-clinostat led to F-actin depolymerization, thinning of fibrillary actin filaments,

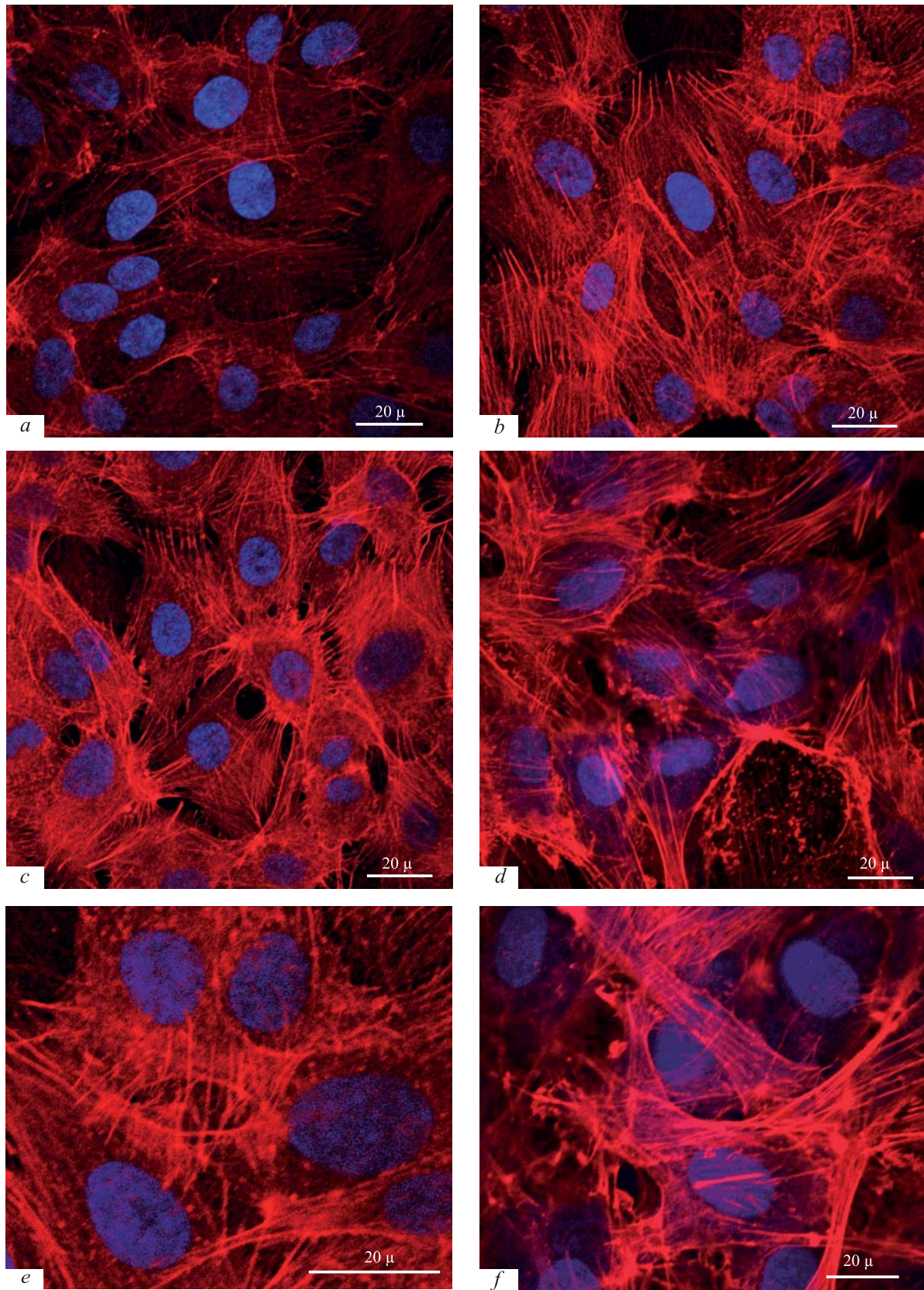


Fig. 3. Changes in the structure of actin cytoskeleton of EC during proinflammatory activation with TNF- α and 24-h RPM exposure. *a*) Static control; *b*) TNF- α -activation; *c*) RPM; *d*) RPM+TNF- α -activation; *e*) formation of filopodia after TNF- α -activation, *f*) formation of lamellae. Fluorescent confocal microscopy.

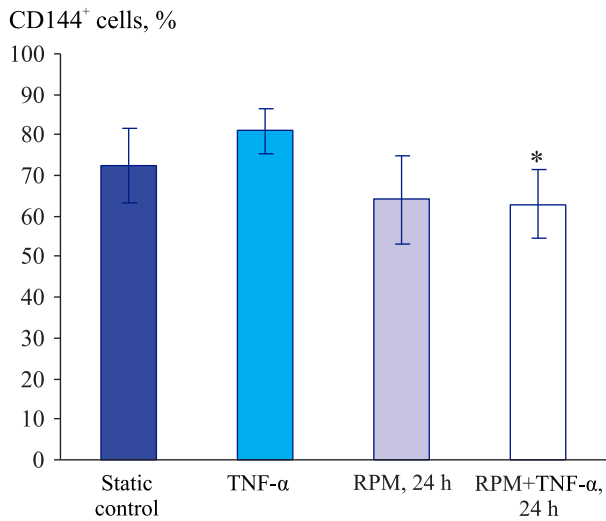


Fig. 4. Number of EC expressing VE-cadherin in under conditions of proinflammatory activation and simulated microgravity. Mean values for 7 experiments are presented. * $p < 0.05$ in comparison with TNF- α -activated cells (Mann–Whitney test).

and their redistribution from the central zone to cell periphery [3,10]. Analysis of intermediate filament and microtubule network showed that microgravity simulation increased the expression of cytokeratin and α -tubulin, thickening of intermediate filament and microtubules, and their redistribution towards the perinuclear space [20].

We compared the state of actin cytoskeleton, morphology, and expression of VE-cadherin in human umbilical cord vein EC under conditions of TNF- α -mediated activation, microgravity simulation, and combined exposure to these factors. Changes occurring in cells during their exposure to RPM largely coincided with those described in published reports. At the same time, the effect of simulated microgravity on TNF- α -activated EC has never been described. We found that proinflammatory activation and 24-h RPM exposure led to the formation of characteristic “emptiness” in the perinuclear space due to clearing of the central zone from microfilaments; the content of de-

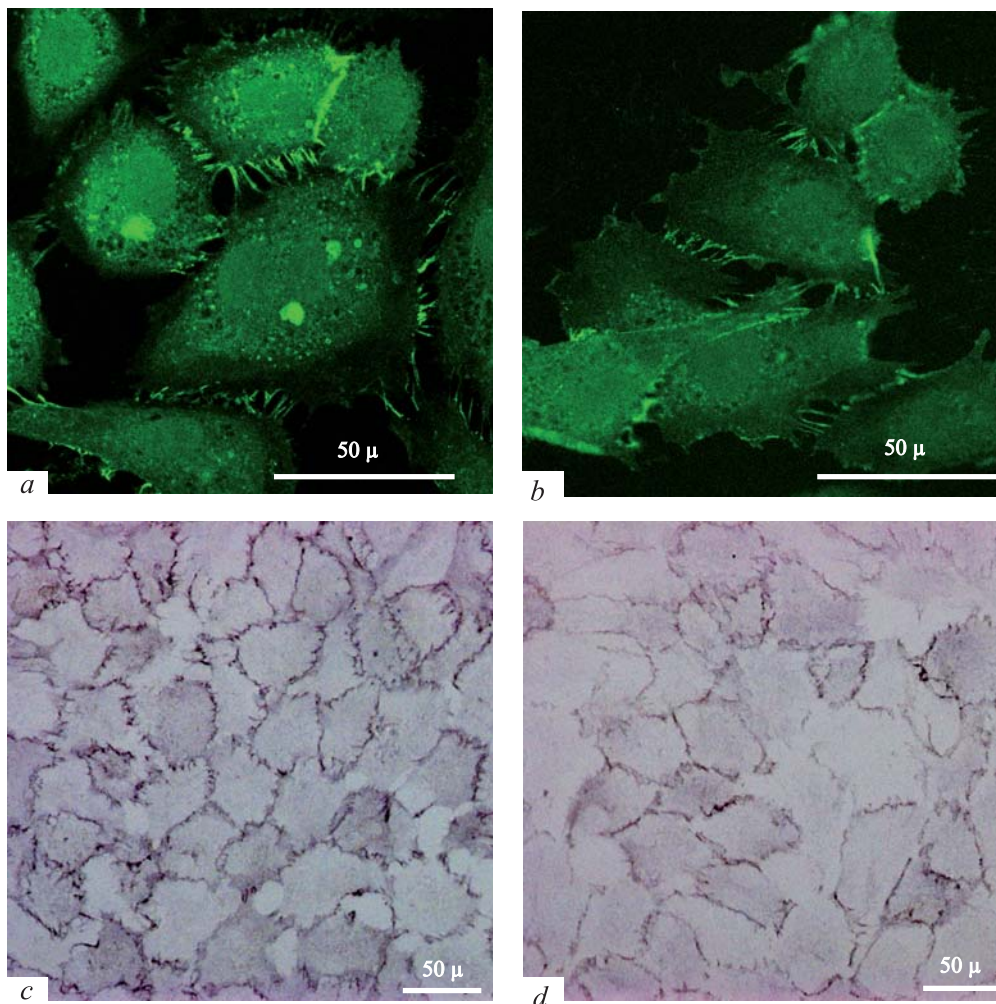


Fig. 5. Expression of VE-cadherin under normal conditions (a, c) and after 6-h (b) and 24-h (d) RPM exposure. Results of indirect immunocytochemical fluorescent staining of VE-cadherin molecule (a, b) (confocal microscopy) and indirect immunohistochemical staining using a DAB Peroxidase kit (c, d) (light microscopy).

polymerized actin significantly increased under these conditions. Rearrangement of actin cytoskeleton was accompanied by changes in EC morphology. For instance, combined exposure to simulated microgravity and proinflammatory activation led to the appearance of clear-cut granularity in the perinuclear cytosol and vacuole-like structures, which could indicate activation of synthetic and secretory activity of these cells.

Actin filaments anchored in certain sites of cell plasmalemma are primarily related to adhesion foci, cell–cell adhesion proteins, membrane proteins, and nuclear membrane. Being dynamic structures, they are capable of rapid rearrangement. However, we cannot assert that microfilament remodeling in response to microgravity exposure observed in our experiments was determined by depolymerization/polymerization of actin fibrils. It was found that TNF- α -induced changes in the architecture of actin cytoskeleton in EC were caused by simple dynamic shift of polymerized F-actin fibrils due to changes in the cell shape [30]. It is quite possible that microgravity induces dynamic shift of actin fibrils.

Signaling pathways mediating remodeling of the actin skeleton under conditions of gravity vector randomization and proinflammatory activation are not quite understood. However, recent studies have shown that changes in the spatial organization of the cytoskeleton and increased cell motility under conditions of simulated microgravity can be related to endothelial NO synthase overexpression and signal transduction mediated by PI3P/Akt-signaling pathway [29]. Moreover, it was hypothesized that Rho GTPases are essential regulators of microfilament reorganization under conditions of simulated microgravity [4,19]. It is also well-known that TNF- α triggers activation of intracellular signal transduction pathways, including those mediated by NF- κ B, c-JNK, and other MAPK [18,39], Rho GTPase family proteins acting as transmitters [11,39]. We can hypothesize that the described effect of proinflammatory activation and simulated microgravity is determined by simultaneous activation of various signaling pathways converging to the common target, Rho GTPase family proteins that regulate cytoskeleton organization.

Thus, microgravity simulation on RPM induces reorganization of the actin cytoskeleton, changes in cell morphology, and inhibition of VE-cadherin expression. In TNF- α -activated EC exposed to 3D-clinostasis, depolymerization of microfilaments was more pronounced. Based on these observations, we can assume that combined exposure to simulated microgravity and proinflammatory activation can lead to pathological dysfunction and enhanced permeability of the endothelial monolayer and metabolic disorders in adjacent tissues.

The study was supported by the Russian Foundation for Basic Research (grant 12-04-31763 mol-a).

REFERENCES

1. A. S. Antonov, A. V. Krushinskii, M. A. Nikolaeva, et al., *Tsitologiya*, **23**, No. 10, 1154-1159 (1981).
2. L. B. Buravkova, *Aviakosm. Ekol. Med.*, **42**, No. 6, 10-18 (2008).
3. L. B. Buravkova and N. V. Merzlikina, *Aviakosm. Ekol. Med.*, **38**, No. 6, 56-61 (2004).
4. M. P. Gershovich, Yu. G. Gershovich, and L. B. Buravkova, *Aviakosm. Ekol. Med.*, **45**, No. 4, 39-41 (2011).
5. Yu. A. Romanov, N. V. Kabaeva, and L. B. Buravkova, *Aviakosm. Ekol. Med.*, **34**, No. 4, 23-26 (2000).
6. Yu. A. Romanov, N. V. Kabaeva, and L. B. Buravkova, *Aviakosm. Ekol. Med.*, **35**, No. 1, 37-40 (2001).
7. K. M. Baldwin, *Med. Sci. Sports Exerc.*, **28**, No. 8, 983-987 (1996).
8. G. Bazzoni and E. Dejana, *Physiol. Rev.*, **84**, No. 3, 869-901 (2004).
9. J. B. Boonyaratanakornkit, A. Cogoli, C. F. Li, et al., *FASEB J.*, **19**, No. 14, 2020-2022 (2005).
10. L. B. Buravkova and Y. A. Romanov, *Acta Astronaut.*, **48**, No. 5-12, 647-650 (2001).
11. S. B. Campos, S. L. Ashworth, S. Wean, et al., *Am. J. Physiol. Renal. Physiol.*, **296**, No. 3, F487-F495 (2009).
12. S. I. Carlsson, M. T. Bertilaccio, E. Ballabio, and J. A. Maier, *Biochim. Biophys. Acta*, **1642**, No. 3, 173-179 (2003).
13. P. Carmeliet, M. G. Lampugnani, L. Moons, et al., *Cell*, **98**, No. 2, 147-157 (1999).
14. S. J. Crawford-Young, *Int. J. Dev. Biol.*, **50**, Nos. 2-3, 183-191 (2006).
15. P. F. Davies and S. C. Tripathi, *Circ. Res.*, **72**, No. 2, 239-245 (1993).
16. J. M. Fritsch-Yelle, U. A. Leuenberger, D. S. D'Aunno, et al., *Am. J. Cardiol.*, **81**, No. 11, 1391-1392 (1998).
17. D. Grimm, J. Bauer, P. Cossmehl, et al., *FASEB J.*, **16**, No. 6, 604-606 (2002).
18. A. Hall, *Science*, **279**, 509-514 (1998).
19. M. Imamizo-Sato, A. Higashibata, and N. Ishioka, *Biol. Sci. Space*, **16**, No. 3, 203-204 (2002).
20. M. Infanger, P. Kossmehl, M. Shakibaei, et al., *Apoptosis*, **11**, No. 5, 749-764 (2006).
21. B. D. Levine, J. H. Zuckerman, and J. A. Pawelczyk, *Circulation*, **96**, No. 2, 517-525 (1997).
22. M. L. Lewis, L. A. Cubano, B. Zhao, et al., *FASEB J.*, **15**, No. 10, 1783-1785 (2001).
23. D. Li, B. Yang, and J. L. Mehta, *Cardiovasc. Res.*, **42**, No. 3, 805-813 (1999).
24. V. Mako, J. Czucz, Z. Weiszhar, et al., *Cytometry, Part A*, **77**, No. 10, 962-970 (2010).
25. C. Michiels, *J. Cell. Physiol.*, **196**, No. 3, 430-443 (2003).
26. F. E. Nwariaku, Z. Liu, X. Zhu, et al., *Blood*, **104**, No. 10, 3214-3220 (2004).
27. J. S. Pober, M. P. Bevilacqua, D. L. Mendrick, et al., *J. Immunol.*, **136**, No. 5, 1680-1687 (1986).
28. D. S. Sangha, S. Han, R. E. Purdy, *J. Appl. Physiol.*, **91**, No. 2, 789-796 (2001).
29. F. Shi, Y. C. Wang, T. Z. Zhao, et al., *PLoS One*, **7**, No. 7, doi: 10.1371/journal.pone.0040365 (2012).

30. K. M. Stroka, J. A. Vaitkus, and H. Aranda-Espinoza, *Eur. Biophys.*, **41**, No. 11, 939-947 (2012).
 31. M. Toborek, S. Barger, M.P. Mattson, *et al.*, *J. Lipid Res.*, **37**, No. 1, 123-135 (1996).
 32. E. Tzima, M. Irani-Tehrani, W. B. Kiosses, *et al.*, *Nature*, **437**, 426-431 (2005).
 33. B. M. Uva, M. A. Masini, M. Sturla, *et al.*, *Brain Res.*, **934**, No. 2, 132-139 (2002).
 34. J. J. W. A. van Loon, J. P. Veldhuijzen, J. Kiss, *et al.*, *Adv. Space Res.*, **39**, No. 7, 1161-1165 (2007).
 35. J. Vassy, S. Portet, M. Beil, *et al.*, *FASEB J.*, **15**, No. 6, 1104-1106 (2001).
 36. P. A. Watson, *FASEB J.*, **5**, No. 7, 2013-2019 (1991).
 37. W. I. Weis and W. J. Nelson, *J. Biol. Chem.*, **281**, No. 47, 35,593-35,597 (2006).
 38. R. White and M. Averner, *Nature*, **409**, 1115-1118 (2001).
 39. B. Wojciak-Stothard, A. Entwistle, R. Garg, AND A. J. Ridley, *J. Cell. Physiol.*, **176**, No. 1, 150-165 (1998).
-
-